ISSN 1070-3284, Russian Journal of Coordination Chemistry, 2013, Vol. 39, No. 1, pp. 11–22. © Pleiades Publishing, Ltd., 2013.
Original Russian Text © P.A. Petrov, T.S. Sukhikh, D.A. Piryazev, A.V. Virovets, S.N. Konchenko, 2013, published in Koordinatsionnaya Khimiya, 2013, Vol. 39, No. 1, pp. 14–25.

Syntheses and Structures of the Cobalt, Nickel, and Zinc Complexes with 1,4-Diaza-1,3-Butadiene Ligands

P. A. Petrov, T. S. Sukhikh, D. A. Piryazev, A. V. Virovets, and S. N. Konchenko*

Nikolaev Institute of Inorganic Chemistry, Siberian Branch, Russian Academy of Sciences,
pr. akademika Lavrent'eva 3, Novosibirsk, 630090 Russia
**e-mail: konch@niic.nsc.ru*

Received January 11, 2012

Abstract—Several cobalt(II), nickel(II), and zinc(II) complexes with a series of ligands of the 1,4-diaza-1,3-butadiene type bearing aryl (2,6-di-*iso*-propylphenyl, mesityl) and alkyl (*tert*-butyl, *iso*-propyl) substituents at the nitrogen atoms are synthesized. The obtained complexes are characterized by X-ray structure analysis, IR spectroscopy, and elemental analysis.

DOI: 10.1134/S1070328413010089

Interest in transition metal complexes with diimine ligands has substantially increased after the discovery by M. Brookhart and coauthors of the catalytic activity of the Ni(II) and Pd(II) complexes with substituted 1,4-diaza-1,3-butadienes (DAB) and their analogs, acetanaphthene-1,2-diimines (BIAN), in the polymerization of α-olefins [1]. Due to the possibility of varying substituents R^1 and R^2 in DAB, several tens of these combinations and their complexes were obtained. It was found soon that similar iron complexes are also catalytically active in the same reactions. Moreover, the substituents at the nitrogen and carbon atoms of the ligand were shown to affect the spin state of the central atom and, as a consequence, the mechanism and degree of polymerization [2, 3]. Then CO and styrene copolymerization [4], hydrosilylation [5], cycloisomerization [6], and other processes were added to the list of reactions catalyzed by the transition metal complexes with DAB or BIAN.

One of the properties of DAB attracting rapt attention is the capability of reversible stepwise reducing to the radical anion and dianion, whereas BIAN can be reduced even to the tetraanion (scheme). This provides the possibility of manifesting the redox activity of complexes even of the metals that are not characterized by several oxidation states. The possibility of different coordination modes of DAB also results in the stabilization of unusual metal–metal bonds, for example, Zn–Zn [7] or the shortest (found at present) Cr–Cr bond (1.8028(9) Å) [8].

In spite of progress in the synthetic chemistry of the complexes with diimine ligands, the majority of the synthesized compounds (even the Ni(II) and Pd(II) complexes of the most representative series) was not characterized by X-ray structure analysis. The number of the described complexes of other metals (in particular, Zn) is much smaller. Therefore, the synthesis and X-ray structure analysis of the same type complexes $[M(^{R1}DAB^{R2})X_2]$ of different transition metals with the same ligand environment are urgent problems. It is important to determine the structures of these complexes for understanding tendencies in changing their catalytic properties.

This work is devoted to the development of methods for the synthesis and systematic X-ray structure analysis of the Co, Ni, and Zn complexes with the group of diimine ligands containing different substituents in the side chain (R^1 = H, R^2 = *iso*-Pr, *tert*-Bu; R^1 = CH_3, R^2 = 2,4,6-$Me_3C_6H_2$ (Mes), 2,6-*iso*-$Pr_2C_6H_3$ (Dipp)).

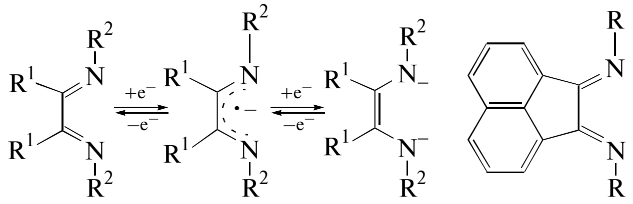

$^{R1}DAB^{R2}$ $(^{R1}DAB^{R2})^-$ $(^{R1}DAB^{R2})^{2-}$ BIAN-R

Scheme.

EXPERIMENTAL

The complexes were synthesized under argon using a standard Schlenk apparatus. The ligands $^{Me}DAB^{Dipp}$ and $^{Me}DAB^{Mes}$ were kindly presented by J. Treptow (Karlsruhe University, Germany). The ligands $^{H}DAB^{tBu}$ and $^{H}DAB^{iPr}$ [9], as well as $[Ni(Dme)Cl_2]$ were synthesized using described procedures [10]. Solvents for the syntheses were dehydrated and degassed by reflux and distillation in an inert atmosphere using the corresponding drying agents [11]. IR spectra were recorded on a SCIMITAR FTS 2000 instrument. Elemental analyses of samples to C, H, and N were carried out on a Euro EA 3000 instrument at the Laboratory of Microanalysis at the Nikolaev Institute of Inorganic Chemistry (Siberian Branch, Russian Academy of Sciences). UV-VIS spectra were recorded on a Gelios Gamma spectrophotometer.

Synthesis of $[Zn(^{Me}DAB^{Dipp})Cl_2]$ (I). Diethyl ether Et_2O (10 mL) was added to a mixture of anhydrous $ZnCl_2$ (0.246 g, 1.80 mmol) and $^{Me}DAB^{Dipp}$ (0.740 g, 1.83 mmol). A yellow solution with a jelly-like yellow precipitate that formed was stirred at ambient temperature for 2 days. The solvent was evaporated to dryness, the product was dissolved in hot tetrahydrofuran (18 mL), and the solution was kept at –18°C for 3 days. A yellow precipitate that formed was separated and washed with ether. The solution was concentrated by evaporation to 1/2 volume, and Et_2O (10 mL) was added. The mixture cooled to –18°C was kept for 6 days. The precipitate was filtered off and washed with Et_2O. The yield was 0.668 g (70%). The crystals suitable for X-ray structure analysis were formed in 7 days from a saturated (at ambient temperature) and cooled to +2°C solution of the complex in MeCN.

^1H NMR ($(CD_3)_2CO$; δ, ppm): 7.36 (s, 3H Ar–H), 3.06 (s, 2H, $C\underline{H}(CH_3)_2$), 2.76 (s, 3H, $N{=}C{-}C\underline{H}_3$), 1.32, 1.13 (2s, 12H, $CH(C\underline{H}_3)_2$). IR (KBr; ν, cm^{-1}): 2964, 2925, 2868, 1654, 1607, 1464, 1443, 1378, 1209, 788. UV-VIS (CH_2Cl_2; λ, nm (ε, L mol^{-1} cm^{-1})): 234 (11000), 358 (800).

For $C_{28}H_{40}N_2Cl_2Zn$

anal. calcd. (%):	C, 62.2;	H, 7.4;	N, 5.2.
Found (%):	C, 61.7;	H, 7.4;	N, 5.1.

Synthesis of $[Zn(^{Me}DAB^{Mes})Cl_2]$ (II). (1) A solution of $ZnCl_2$ (0.098 g, 0.72 mmol) in tetrahydrofuran (10 mL) was added to $^{Me}DAB^{Mes}$ (0.254 g, 0.792 mmol). A yellow jelly-like precipitate was formed immediately, and the solution turned yellow. The mixture was refluxed with a reflux condenser for 6 h. The solvent was evaporated to dryness, the residue was dissolved in MeCN (7 mL), Et_2O (10 mL) was added, and the mixture was cooled to +2°C. After 4 days, the yellow crystals that formed were filtered off and washed with Et_2O. The yield was 0.327 g (57%).

(2) Tetrahydrofuran (10 mL) was added to a mixture of anhydrous $CrCl_3$ (0.104 g, 0.656 mmol), $^{Me}DAB^{Mes}$ (0.197 g, 0.616 mmol), and zinc dust (0.025 g, 0.38 mmol). The mixture was refluxed for 8 h. The obtained brown solution was kept at +2°C for several days. Yellow-green transparent crystals suitable for X-ray structure analysis were formed, filtered, and washed with Et_2O. The yield was ~5%.

^1H NMR (CD_2Cl_2; δ, ppm): 7.02 (s, 4H Ar–H), 2.33 (s, 6H, $Ar{-}CH_3$), 2.30 (s, 6H, $N{=}C{-}CH_3$), 2.22 (s, 12H, $Ar{-}CH_3$). ^{13}C NMR (CD_2Cl_2; δ, ppm): 169.78 (s, N=C), 139.75 (s, Ar–*i*-C), 137.11 (s, Ar–*p*-C), 129.56 (s, Ar–*m*-C), 127.93 (s, Ar–*o*-C), 20.52 (s, Ar–*p*-CH_3), 18.57 (s, Ar–*o*-CH_3), 18.02 (s, $N{=}C{-}CH_3$). IR (KBr; ν, cm^{-1}): 2968, 2920, 2859, 1647, 1598, 1479, 1443, 1373, 1228, 854. UV-VIS (CH_2Cl_2; λ, nm (ε, L mol^{-1} cm^{-1})): 235 (8000), 267 (1100), 374 (500).

For $C_{22}H_{28}N_2Cl_2Zn$

anal. calcd. (%):	C, 57.8;	H, 6.1;	N, 6.1.
Found (%):	C, 58.0;	H, 6.3;	N, 6.1.

Synthesis of $[Zn(^{H}DAB^{tBu})Cl_2]$ (III). Tetrahydrofuran (15 mL) was added to a mixture of anhydrous $ZnCl_2$ (0.274 g, 2.01 mmol) and $^{H}DAB^{tBu}$ (0.372 g, 2.21 mmol). A white precipitate was immediately formed. The mixture was stirred at ambient temperature for 5 h, then the solvent was evaporated to dryness, and the residue was dissolved in CH_2Cl_2. The slow diffusion of Et_2O to this solution resulted in the formation of crystals suitable for X-ray structure analysis. The yield was 0.612 g (70%).

^1H NMR ($(CD_3)_2CO$; δ, ppm): 8.50 (s, 2H, CH), 1.50 (s, 18H, CH_3). ^{13}C NMR ($(CD_3)_2CO$; δ, ppm): 156.7 (s, CH), 61.5 (s, $\underline{C}(CH_3)_3$), 29.5 (s, CH_3). IR (KBr; ν, cm^{-1}): 2977, 2932, 1662, 1598, 1473, 1386, 1244, 1205, 992, 901. UV-VIS (CH_2Cl_2; λ, nm (ε, L mol^{-1} cm^{-1})): 235 (9400).

For $C_{10}H_{20}N_2Cl_2Zn$

anal. calcd. (%):	C, 39.4;	H, 6.6;	N, 9.2.
Found (%):	C, 39.5;	H, 6.5;	N, 9.2.

Synthesis of $[Zn(^{H}DAB^{iPr})Cl_2]$ (IV). Anhydrous $ZnCl_2$ (0.135 g, 0.99 mmol) was dissolved in Et_2O (5 mL), and the obtained solution was added to a solution of $^{H}DAB^{iPr}$ (0.150 g, 1.07 mmol) in Et_2O (5 mL). A milk-white jelly-like precipitate was immediately formed. Methylene chloride (7 mL) was added to the complete dissolution of the precipitate. Crystals suitable for X-ray structure analysis were formed in 4 days from the solution cooled to +2°C. The yield was 0.095 g (35%).

IR (KBr; ν, cm^{-1}): 2976, 2932, 2874, 1655, 1595, 1464, 1402, 1383, 1310, 1157, 1127, 993, 909.

For $C_8H_{16}N_2Cl_2Zn$

anal. calcd. (%):	C, 34.7;	H, 5.8;	N, 10.1.
Found (%):	C, 34.9;	H, 5.8;	N, 10.1.

Synthesis of $[Co(^{Me}DAB^{Dipp})Cl_2]$ (V). Tetrahydrofuran (15 mL) was added to a mixture of anhydrous $CoCl_2$ (0.452 g, 3.48 mmol) and $^{Me}DAB^{Dipp}$ (1.415 g, 3.502 mmol). The mixture was refluxed for 12 h. A blue precipitate was dissolved, and a dark green solution with a green precipitate was formed. The mixture was cooled to −18°C. After 6 days the precipitate was filtered off and washed with ether. The yield was 1.510 g (80%). The product was purified by recrystallization from a MeCN–Et_2O mixture.

IR (KBr; ν, cm^{-1}): 2962, 2924, 2867, 1641, 1588, 1464, 1442, 1379, 1209, 788. UV-VIS (CH_2Cl_2; λ, nm (ε, L mol^{-1} cm^{-1})): 310 (1765), 591 (127), 658 (127), 711 (313).

For $C_{28}H_{40}N_2Cl_2Co$

anal. calcd. (%):	C, 62.9;	H, 7.5;	N, 5.2.
Found (%):	C, 61.9;	H, 7.4;	N, 5.1.

Synthesis of $[Co(^{Me}DAB^{Mes})Cl_2]$ (VI). Methylene chloride (30 mL) was added to a mixture of anhydrous $CoCl_2$ (0.147 g, 1.13 mmol) and $^{Me}DAB^{Me}$ (0.394 g, 1.23 mmol). The mixture was stirred at ambient temperature. A blue precipitate was dissolved, and a dark green solution with a green precipitate was formed. The precipitate was filtered off and purified by recrystallization from CH_2Cl_2 followed by washing of the crystals with Et_2O. The solution was cooled to −18°C. After a day the crystals that formed were filtered off, washed with Et_2O, and dried. The yield was 0.360 g (70%). The crystals suitable for X-ray structure analysis were grown by the slow diffusion of Et_2O to a solution of the complex in MeCN.

IR (KBr; ν, cm^{-1}): 2964, 2918, 2859, 1640, 1597, 1477, 1374, 1231, 856. UV-VIS (CH_2Cl_2; λ, nm (ε, L mol^{-1} cm^{-1})): 298 (2900), 404 (1100), 600 (180), 658 (180), 705 (450).

For $C_{22}H_{28}N_2Cl_2Co$

anal. calcd. (%):	C, 58.7;	H, 6.2;	N, 6.2.
Found (%):	C, 58.8;	H, 6.3;	N, 6.2.

Synthesis of $[Co(^{H}DAB^{tBu})Cl_2]$ (VII). The product was obtained from $CoCl_2$ and $^{H}DAB^{tBu}$ using the same method as that for complex **V**. The yield was 50%.

IR (KBr; ν, cm^{-1}): 2975, 2903, 1648, 1593, 1472, 1384, 1243, 1205, 990, 897.

For $C_{10}H_{20}N_2Cl_2Co$

anal. calcd. (%):	C, 40.2;	H, 6.7;	N, 9.4.
Found (%):	C, 40.4;	H, 6.7;	N, 9.3.

Synthesis of $[Co(^{H}DAB^{iPr})Cl_2]_2$ (VIII). Tetrahydrofuran (THF) (10 mL) was added to a mixture of anhydrous $CoCl_2$ (0.178 g, 1.37 mmol) and $^{H}DAB^{iPr}$ (0.206 g, 1.47 mmol). The mixture was stirred for 30 min at ambient temperature. After the complete dissolution of the reactants, the solvent was evaporated to dryness and the residue was dissolved in MeCN. A double volume of Et_2O was added, and the mixture was kept at +2°C. The yield was 0.16 g (45%).

IR (KBr; ν, cm^{-1}): 2975, 2876, 2718, 2611, 2507, 1650, 1598, 1463, 1400, 1367, 1173, 1136, 1014, 910.

For $C_{16}H_{32}N_4Cl_4Co_2$

anal. calcd. (%):	C, 35.5;	H, 5.9;	N, 10.4.
Found (%):	C, 35.4;	H, 5.6;	N, 10.2.

Synthesis of $[Ni(^{Me}DAB^{Dipp})Cl_2]$ (IX). Acetonitrile (10 mL) was added to a mixture of anhydrous $NiCl_2$ (0.067 g, 0.52 mmol) and $^{Me}DAB^{Dipp}$ (0.386 g, 0.955 mmol), the mixture was refluxed for 4 h, and a dark brown solution with a light yellow precipitate was formed. The solution was filtered, the solvent was evaporated to dryness, and the residue was dissolved in CH_2Cl_2 (10 mL). The crystals suitable for X-ray structure analysis were grown by the slow diffusion of Et_2O to this solution. The yield was 0.040 g (15%).

IR (KBr; ν, cm^{-1}): 2963, 2924, 2867, 1641, 1585, 1464, 1442, 1381, 1212, 789. UV-VIS (CH_2Cl_2; λ, nm (ε, L mol^{-1} cm^{-1})): 240 (17 000), 311 (5300), 365 (2433), 421 (832).

For $C_{28}H_{40}N_2Cl_2Ni$

anal. calcd. (%):	C, 62.8;	H, 7.5;	N, 5.2.
Found (%):	C, 63.1;	H, 7.5;	N, 5.2.

Synthesis of $[Ni(^{Me}DAB^{Mes})Cl_2]$ (X). The product was obtained similarly to complex **IX**. The crystals suitable for X-ray structure analysis were grown by the slow diffusion of Et_2O to a solution of the complex in CH_2Cl_2. The yield was 85%.

IR (KBr; n, cm–1): 3000, 2953, 2918, 2859, 1647, 1587, 1476, 1376, 1233, 856.

For $C_{22}H_{28}N_2Cl_2Ni$

anal. calcd. (%):	C, 58.6;	H, 6.2;	N, 6.2.
Found (%):	C, 58.6;	H, 6.1;	N, 6.2.

Synthesis of $[Ni(^{H}DAB^{tBu})Cl_2]_2$ (XI). The product was obtained similarly to complex **IX**. The yield was 55%. The crystals suitable for X-ray structure analysis were grown by the slow diffusion of Et_2O to a solution of the complex in CH_2Cl_2.

IR (KBr; ν, cm^{-1}): 2974, 2929, 2874, 1659, 1607, 1480, 1384, 1367, 1226, 1212, 996, 889. UV-VIS (CH_2Cl_2; λ, nm (ε, L mol^{-1} cm^{-1})): 233 (14 000), 253 (9600), 296 (4300), 386 (1100).

For $C_{20}H_{40}N_4Cl_4Ni_2$

anal. calcd. (%):	C, 40.3;	H, 6.7;	N, 9.4.
Found (%):	C, 39.8;	H, 6.8;	N, 9.2.

Synthesis of $[Ni_2(^{H}DAB^{iPr})_2(THF)Cl_4]$ (XII). $^{H}DAB^{iPr}$ (0.199 g, 1.42 mmol) was added to a suspension of $[Ni(Dme)Cl_2]$ (Dme is 1,2-dimethoxyethane) (0.312 g, 1.42 mmol) in THF (25 mL). The solution turned reddish, and a green-yellow precipitate was formed. After 3 h of stirring at ambient temperature, the mixture was heated to boiling and the solution was filtered and cooled to +2°C. The yellow-green crystals suitable for X-ray structure analysis were formed in 2 days. They were filtered off and dried. The solid residue obtained in the previous filtration was joined with the mother liquor and crystallized similarly. The total yield was 0.200 g (46%).

IR (KBr; ν, cm^{-1}): 2972, 2932, 2874, 1660, 1630, 1608, 1465, 1401, 1366, 1323, 1261, 1172, 1134, 1070, 1037, 1021, 920, 879, 802. UV-VIS (CH_2Cl_2; λ, nm (ε, L mol^{-1} cm^{-1})): 236 (9200), 290 (1600), 361 (220).

For $C_{20}H_{40}N_4OCl_4Ni_2$			
anal. calcd. (%):	C, 39.5;	H, 6.6;	N, 9.2.
Found (%):	C, 38.9;	H, 6.6;	N, 8.2.

Synthesis of $[Ni_3(^{H}DAB^{iPr})_3Cl_5]_2[Ni_4(^{H}DAB^{iPr})_2(MeCN)_2Cl_{10}]$ (XIII). Methylene chloride (15 mL) was added to a mixture of $[Ni(Dme)Cl_2]$ (0.312 g, 1.42 mmol) and $^{H}DAB^{iPr}$ (0.202 g, 1.44 mmol). The solution turned brown, and a green-yellow precipitate was formed. After stirring the solution at ambient temperature, the precipitate turned green within a day. The precipitate was separated and dried in vacuo and then dissolved in MeCN. The green crystals suitable for X-ray structure analysis were grown by the slow diffusion of Et_2O to this solution. The yield was 0.090 g (25%).

IR (KBr; ν, cm^{-1}): 2972, 2933, 2873, 1623, 1466, 1401, 1367, 1327, 1174, 1135, 1020, 898. UV-VIS (CH_2Cl_2; λ, nm (ε, L mol^{-1} cm^{-1})): 235 (50000), 291 (9200), 362 (1000).

For $C_{72}H_{140}N_{20}Cl_{20}Ni_{10}$			
anal. calcd. (%):	C, 33.7;	H, 5.5;	N, 10.9.
Found (%):	C, 33.8;	H, 5.8;	N, 10.5.

X-ray structure analysis. The crystallographic and X-ray diffraction data for the determination of structures of 12 compounds were obtained on a Bruker X8 Apex CCD automated diffractometer (graphite monochromator, $\lambda(MoK_\alpha) = 0.71073$ Å). An absorption correction was applied semiempirically using the SADABS program [12]. The structures were solved by a direct method and refined by least squares in the anisotropic approximation (SHELXTL) [13]. Hydrogen atoms were localized geometrically and refined in the rigid body approximation. A crystal of compound **XII** is a pseudomerohedral twin with the weight of the main component 61.8%. The twinning matrix (0 1 0/1 0 0/0 0 1) was used for refinement. The structures of compounds **VI** and **X** are chiral with the Fleck parameters 0.002(7) and 0.003(8), respectively. The most important crystallographic data and refinement parameters of the structures are given in Tables 1 and 2. Selected bond lengths and angles are listed in Tables 3–5. The coordinates of non-hydrogen atoms were deposited with the Cambridge Crystallographic Data Centre (nos. 857852–857863 for compounds **I–IV** and **VI–XIII**, respectively; deposit@ccdc.cam. ac.uk or http://www.ccdc. cam.ac.uk/data_request/cif) and can be available from the authors.

RESULTS AND DISCUSSION

As it was found, the interaction of solutions of $ZnCl_2$ and the ligand in diethyl ether or THF at ambient temperature is a convenient method for the synthesis of the Zn(II) derivatives. Already several minutes after, light yellow precipitates of complexes **I–IV** began to form. After recrystallization, the yields of the products ranged from 35 to 75%. Single crystals suitable for X-ray structure analysis were obtained by cooling solutions of the complexes in CH_2Cl_2, THF, or MeCN.

Complex **II** was also isolated when attempting to obtain the Cr(II) complex with the diimine ligand using Zn as a reducing agent. The reaction of $CrCl_3$ with $^{Me}DAB^{Mes}$ and zinc dust affords a solution from which complex **II** was isolated in the crystalline form on cooling in 5% yield. No chromium complex was observed in the reaction mixture. The synthesis of the diamagnetic chromium complexes of stoichiometry $[CrLCl_2]$ (L = $^{Me}DAB^{Mes}$, $^{Me}DAB^{Dipp}$, BIAN-Dipp, BIAN-C_6H_4-*o*-Me) obtained by the reaction of $[Cr(THF)_3Cl_3]$, $^{Me}DAB^{Mes}$, and Zn in a ratio of 1 : 3 : 5 has earlier been reported [14]. However, it has been shown later than the compounds isolated [14] are the Zn complexes [15].

The Co(II) complexes (**V–VIII**) were obtained by reflux of anhydrous $CoCl_2$ and ligand (1 : 1) in THF or MeCN followed by the recrystallization of the product from CH_2Cl_2. Single crystals suitable for X-ray structure analysis were grown on cooling of a solution of the complex in CH_2Cl_2 or by the slow diffusion of Et_2O to solutions in MeCN. The obtained complexes are stable in air and can be stored without decomposition for a prolonged time, except for $[Co(^{H}DAB^{iPr})Cl_2]_2$ (**VIII**), which decomposes within several weeks. The use of $CoCl_2 \cdot 6H_2O$ as the starting substance results only in the formation of complexes containing no DAB. The reflux of $CoCl_2 \cdot 6H_2O$ with $^{Me}DAB^{Me}$ (1 : 1) in MeCN affords molecular $[Co(MeCN)_4(H_2O)_2]Cl_2$ [16], whereas the same reaction in THF affords the chain polymer complex $[\{Co_4(\mu\text{-}Cl)_6Cl_2(THF)_4(H_2O)_2\} \cdot 2THF]_\infty$ [17]. The

Table 1. Crystallographic data and refinement parameters for structures **I–IV**, **VI**, and **VII**

Parameter	Value					
	I · CH_3CN	**II** · C_4H_8O	**III**	**IV**	**VI**	**VII**
Empirical formula	$C_{30}H_{43}Cl_2N_3Zn$	$C_{26}H_{36}Cl_2N_2OZn$	$C_{10}H_{20}Cl_2N_2Zn$	$C_8H_{16}Cl_2N_2Zn$	$C_{22}H_{28}Cl_2CoN_2$	$C_{10}H_{20}Cl_2CoN_2$
FW	581.94	528.84	304.55	276.50	450.29	298.11
Crystal system; space group	Orthorhombic, *Pnma*	Monoclinic, $P2_1/c$	Monoclinic, $P2_1/n$	Monoclinic, $C2/c$	Orthorhombic, $P2_12_12_1$	Monoclinic, $P2_1/n$
Temperature, K	100.0(2)	91.0(2)	100.0(2)	100.0(2)	100.0(2)	91.0(2)
a, Å	17.4595(6)	12.9137(4)	6.9851(2)	9.6280(4)	13.9052(2)	6.9939(3)
b, Å	17.5776(5)	14.2762(4)	10.0439(3)	11.7190(5)	14.4210(2)	10.0302(6)
c, Å	9.8944(3)	14.3954(5)	20.1573(6)	11.1482(5)	22.9247(5)	20.1505(12)
α, deg	90	90	90	90	90	90
β, deg	90	90.766(1)	95.211(1)	102.657(2)	90	95.130(2)
γ, deg	90	90	90	90	90	90
V, Å^3	3036.55(16)	2653.68(14)	1408.34(7)	1227.29(9)	4597.02(14)	1407.90(13)
Z	4	4	4	4	8	4
μ, mm^{-1}	1.007	1.147	2.097	2.398	0.988	1.572
F(000)	1232	1112	632	568	1880	620
Crystal size, mm	0.29 × 0.15 × 0.09	0.62 × 0.15 × 0.13	0.89 × 0.15 × 0.14	0.41 × 0.28 × 0.20	0.51 × 0.33 × 0.08	0.55 × 0.06 × 0.05
θ Range, deg	2.32–31.46	2.01–31.35	2.27–32.13	2.78–32.54	1.67–31.33	2.03–25.68
Ranges of indices h, k, l	$-15 \le h \le 23$, $-22 \le k \le 16$, $-13 \le l \le 13$	$-18 \le h \le 14$, $-19 \le k \le 14$, $-20 \le l \le 20$	$-9 \le h \le 10$, $-13 \le k \le 13$, $-28 \le l \le 29$	$-14 \le h \le 10$, $-16 \le k \le 15$, $-15 \le l \le 14$	$-20 \le h \le 12$, $-20 \le k \le 18$, $-27 \le l \le 33$	$-6 \le h \le 8$, $-12 \le k \le 12$, $-24 \le l \le 23$
T_{min}, T_{max}	0.689, 0.913	0.719, 0.860	0.637, 1	0.811, 1	0.802, 1	0.561, 1
Number of measured/independent/observed ($I > 2\sigma(I)$) reflections	16533/4085/2975	20368/7164/5732	18201/4225/4022	7792/1859/1768	33460/12902/11027	9518/2569/1955
R_{int}	0.042	0.023	0.026	0.018	0.028	0.0520
R ($F^2 > 2\sigma(F^2)$), wR (F^2), S	0.035, 0.082, 1.02	0.029, 0.068, 1.02	0.016, 0.062, 1.21	0.021, 0.051, 1.01	0.035, 0.069, 0.95	0.0487, 0.0805, 1.074
Number of refined parameters	173	297	142	133	503	142
$\Delta\rho_{max}/\Delta\rho_{min}$, e Å^{-3}	0.43/–0.38	0.44/–0.39	0.51/–0.41	0.84/–0.88	0.44/–0.34	0.844/–0.628

Table 2. Crystallographic data and refinement parameters for structures **VIII–XIII**

Parameter	Value					
	VIII	**IX**	**X**	**XI**	**XII** · $0.25C_4H_8O$	**XIII** · $2CH_3CN$
Empirical formula	$C_{16}H_{32}Cl_4Co_2N_4$	$C_{28}H_{40}Cl_2N_2Ni$	$C_{22}H_{28}Cl_2N_2Ni$	$C_{10}H_{20}Cl_2N_2Ni$	$C_{21}H_{42}C_9N_4Ni_2O_{1.25}$	$C_{72}H_{140}Cl_{20}N_{20}Ni_{10}$
FW	540.12	534.23	450.07	297.89	629.81	2582.14
Crystal system, space group	Triclinic, $P\bar{1}$	Orthorhombic, *Pnma*	Orthorhombic, $P2_12_12_1$	Monoclinic, $P2_1/c$	Orthorhombic, $P2_12_12$	Triclinic, $P\bar{1}$
Temperature, K	91.0(2)	100.0(2)	100.0(2)	100.0(2)	150.0(2)	150.0(2)
a, Å	6.9794(2)	12.5931(4)	13.9427(2)	10.4905(6)	22.5050(8)	10.8580(5)
b, Å	9.1143(2)	21.2318(9)	14.3282(3)	12.9274(8)	22.5114(8)	13.8773(4)
c, Å	10.1743(2)	10.3448(4)	22.8388(4)	20.7810(13)	12.2478(5)	20.6822(9)
α, deg	79.532(1)	90	90	90	90	77.146(1)
β, deg	73.917(1)	90	90	103.270(2)	90	76.237(1)
γ, deg	71.936(1)	90	90	90	90	69.700(1)
V, Å^3	587.97(2)	2765.93(18)	4562.59(14)	2743.0(3)	6205.0(4)	2805.2(2)
Z	1	4	8	8	8	1
μ, mm^{-1}	1.873	0.913	1.093	1.778	1.578	2.159
F(000)	278	1136	1888	1248	2640	1332
Crystal size, mm	0.34 × 0.17 × 0.17	0.39 × 0.09 × 0.07	0.32 × 0.31 × 0.08	0.34 × 0.11 × 0.09	0.36 × 0.35 × 0.25	0.18 × 0.13 × 0.09
θ Range, deg	2.09–32.22	1.92–31.28	1.78–31.56	1.87–31.31	0.90–31.42	2.03–32.42
Ranges of indices *h*, *k*, *l*	$-9 \le h \le 9$, $-11 \le k \le 12$, $-13 \le l \le 13$	$-10 \le h \le 16$, $-30 \le k \le 25$, $-10 \le l \le 14$	$-16 \le h \le 14$, $-20 \le k \le 12$, $-33 \le l \le 32$	$-15 \le h \le 9$, $-16 \le k \le 17$, $-28 \le l \le 29$	$-30 \le h \le 26$, $-31 \le k \le 28$, $-16 \le l \le 16$	$-15 \le h \le 16$, $-12 \le k \le 20$, $-30 \le l \le 29$
T_{min}, T_{max}	0.821, 1	0.778, 0.94	0.730, 1	0.724, 1	0.663, 1	0.705, 0.823
Number of measured/independent/observed ($I > 2\sigma(I)$) reflections	7207/3193/2857	13925/3857/2615	29569/11433/9112	18640/7528/4987	44215/16426/10474	32739/15363/9436
R_{int}	0.020	0.047	0.036	0.040	0.050	0.049
R ($F^2 > 2\sigma(F^2)$), wR (F^2), S	0.021, 0.050, 1.04	0.039, 0.082, 1.02	0.035, 0.068, 0.93	0.052, 0.136, 1.00	0.053, 0.145, 0.97	0.045, 0.085, 0.94
Number of refined parameters	122	159	503	283	598	568
$\Delta\rho_{max}/\Delta\rho_{min}$, e Å^{-3}	0.40/–0.28	0.46/–0.46	0.39/–0.38	4.03/–0.60	0.88/–0.65	0.49/–0.51

Table 3. Selected interatomic distances and angles in molecules of the complexes in structures **I–IV** and **VI**

I · CH_3CN	**II** · C_4H_8O	**III**	**IV**	**VI**	
		Bond; *d*, Å			
Zn(1)–Cl(1) 2.2085(7)	Zn(1)–Cl(1) 2.2055(4)	Zn(1)–Cl(1) 2.2163(3)	Zn(1)–Cl(1) 2.2095(4)	Co(1)–Cl(1) 2.2216(5)	Co(2)–Cl(3) 2.2336(5)
Zn(1)–Cl(2) 2.2026(8)	Zn(1)–Cl(2) 2.2130(4)	Zn(1)–Cl(2) 2.2110(3)		Co(1)–Cl(2) 2.2291(5)	Co(2)–Cl(4) 2.2102(6)
Zn(1)–N(1) 2.0873(15)	Zn(1)–N(1) 2.0647(12)	Zn(1)–N(1) 2.0754(8)	Zn(1)–N(1) 2.0754(10)	Co(1)–N(1) 2.0358(16)	Co(2)–N(3) 2.0423(16)
	Zn(1)–N(2) 2.0699(12)	Zn(1)–N(2) 2.0825(9)		Co(1)–N(2) 2.0538(16)	Co(2)–N(4) 2.0464(16)
		Angle, deg			
Cl(1)Zn(1)Cl(2) 116.73(3)	Cl(1)Zn(1)Cl(2) 116.568(16)	Cl(1)Zn(1)Cl(2) 115.254(10)	Cl(1)Zn(1)Cl(1)' 121.47(3)	Cl(1)Co(1)Cl(2) 112.63(2)	Cl(3)Co(2)Cl(4) 113.05(2)
N(1)Zn(1)N(1)' 77.67(8)	N(1)Zn(1)N(2) 78.89(5)	N(1)Zn(1)N(2) 81.10(3)	N(1)Zn(1)N(1)' 80.35(5)	N(1)Co(1)N(2) 79.54(6)	N(3)Co(2)N(4) 80.06(6)

both products were identified by the unit cell parameters of the single crystal.

Various sources of the metal were used for the synthesis of the nickel complexes. Reflux of a mixture of anhydrous $NiCl_2$ and ligand in a ratio of 1 : 1 in MeCN results in the disappearance of the starting chloride and the formation of a lemon-yellow precipitate presumably representing mixed acetonitrile–chloride nickel(II) complexes. After this precipitate was filtered off from the solution, the solution was concentrated by evaporation, and the solid residue was recrystallized, the following complexes were obtained in moderate yields: $[Ni(^{Me}DAB^{Dipp})Cl_2]$ (**IX**), $[Ni(^{Me}DAB^{Mes})Cl_2]$ (**X**), and $[Ni(^{H}DAB^{tBu})Cl_2]_2$ (**XI**). We failed to obtain the complexes with $^{H}DAB^{iPr}$ by this method.

The reactions of $[Ni(Dme)Cl_2]$ with $^{H}DAB^{iP}$ give different products, depending on the conditions. Reflux of a mixture of $[Ni(Dme)Cl_2]$ with $^{H}DAB^{iPr}$ in THF affords the binuclear complex $[Ni_2(\mu\text{-}Cl)_3(^{H}DAB^{iPr})_2(THF)Cl] \cdot 0.25THF$ (**XII** · 0.25THF), whereas the reaction in THF or CH_2Cl_2 and crystallization from an acetonitrile–Et_2O mixture result in $[Ni_3(\mu_3\text{-}Cl)_2(\mu\text{-}Cl)_3(^{H}DAB^{iPr})_3]_2[Ni_2(\mu\text{-}Cl)_2(^{H}DAB^{iPr})_2(CH_3CN)_2(NiCl_4)_2] \cdot MeCN$ (**XIII** · MeCN). The cationic part of compound **XIII** is the trinuclear complex $[Ni_3(\mu_3\text{-}Cl)_2(\mu\text{-}Cl)_3(^{H}DAB^{iPr})_3]^+$ (**XIIIa**) in which two μ_3-Cl ligands are coordinated to the Ni_3 triangle and each edge is coordinated by the μ-Cl ligand. The anionic part $[Ni_2(\mu\text{-}Cl)_2(^{H}DAB^{iPr})_2(CH_3CN)_2(NiCl_4)_2]^{2-}$ (**XIIIb**) can be presented as a dimeric complex with two chloride bridges in which the terminal ligands $^{H}DAB^{iPr}$ and MeCM are additionally coordinated to each nickel atom. In addition, the anionic complex $NiCl_4^{2-}$ acts as a terminal ligand in this case.

The synthesized compounds were characterized by IR and UV-VIS spectroscopy. The coordination of the ligand shifts the absorption bands of the multiple bonds (1700–1400 cm^{-1}). In addition, the coordination of $^{Me}DAB^{Mes}$ results in the appearance of an additional absorption band of the complex at approximately 1590–1600 cm^{-1}, which is absent from the spectrum of the free ligand. Diamagnetic zinc complexes **I–III** were characterized by the NMR method. The signals in the ^{13}C NMR spectrum of complex **II**

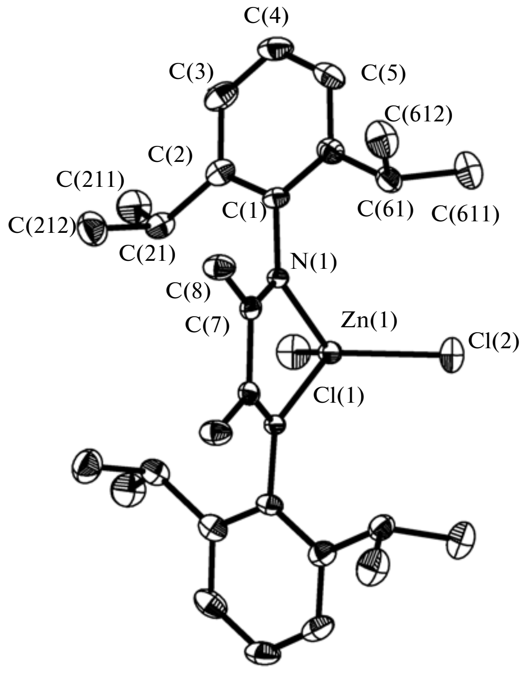

Fig. 1. Structure of complex **I** with the enumeration of atoms (independent part); hydrogen atoms are omitted.

Table 4. Selected interatomic distances and angles in molecules of the complexes in structures **VII–XI**

VII	**VIII**	**IX**	**X**	**XI**
		Bond; *d*, Å		
	Co(1)–Co(1)' 3.5563(2)			Ni(1)–Ni(2) 3.5988(6)
	Co(1)–Cl(2) 2.3913(3)			Ni(1)–Cl(2) 2.2912(9)
	Co(1)–Cl(2)' 2.4198(3)			Ni(2)–Cl(4) 2.2930(9)
Co(1)–Cl(1) 2.2243(10)	Co(1)–Cl(1) 2.2851(4)	Ni(1)–Cl(1) 2.1879(8)	Ni(1)–Cl(1) 2.2211(7)	Ni(1)–Cl(1) 2.3769(9)
Co(1)–Cl(2) 2.2247(10)		Ni(1)–Cl(2) 2.2138(8)	Ni(1)–Cl(1) 2.2211(7)	Ni(1)–Cl(3) 2.3960(9)
			Ni(1)–Cl(3) 2.2037(7)	Ni(2)–Cl(1) 2.3946(9)
			Ni(2)–Cl(2) 2.2061(7)	Ni(2)–Cl(3) 2.3756(9)
			Ni(2)–Cl(4) 2.2253(7)	
Co(1)–N(1) 2.054(3)	Co(1)–N(1) 2.1014(10)	Ni(1)–N(1) 2.0010(15)	Ni(1)–N(1) 1.9938(18)	Ni(1)–N(1*B*) 2.054(3)
Co(1)–N(2) 2.063(3)	Co(1)–N(2) 2.0829(11)		Ni(1)–N(2) 1.9944(19)	Ni(1)–N(2*B*) 2.056(3)
			Ni(2)–N(3) 1.9987(18)	Ni(2)–N(1*A*) 2.054(3)
			Ni(2)–N(4) 1.9894(19)	Ni(2)–N(2*A*) 2.050(3)
		Angle, deg		
Cl(1)Co(1)Cl(2) 113.14(4)	Cl(1)Co(1)Cl(2) 125.837(14)	Cl(1)Ni(1)Cl(2) 118.84(3)	Cl(1)Ni(1)Cl(3) 118.60(3)	Cl(1)Ni(1)Cl(3) 82.06(3)
	Cl(1)Co(1)Cl(2)' 102.434(13)		Cl(2)Ni(2)Cl(4) 119.67(3)	Cl(1)Ni(1)Cl(2) 155.75(3)
	Cl(2)Co(1)Cl(2) 84.676(12)			Cl(2)Ni(1)Cl(3) 92.57(3)
				Cl(1)Ni(2)Cl(3) 82.12(3)
				Cl(1)Ni(2)Cl(4) 92.42(3)
				Cl(3)Ni(2)Cl(4) 156.70(3)
N(1)Co(1)N(2) 81.75(11)	N(1)Co(1)N(2) 77.75(4)	N(1)Ni(1)N(1)' 80.15(9)	N(1)Ni(1)N(2) 80.69(8)	N(1*B*)Ni(1)N(2*B*) 81.23(10)
			N(3)Ni(2)N(4) 80.36(8)	N(1*A*)Ni(2)N(2*A*) 81.17(10)
	Co(1)Cl(2)Co(1)' 95.324(12)			Ni(1)Cl(1)Ni(2) 97.91(3)

Table 5. Selected interatomic distances and angles in complexes **XII** and **XIII**

$\mathbf{XII}\cdot 0.25C_4H_8O$		**XIIIa**	**XIIIb**
Bond; *d*, Å			
Ni(1)–Ni(2)3.0632(15)	Ni(3)–Ni(4)3.0527(13)	Ni(1)–Ni(2) 3.123(1)	Ni(4)–Ni(4)' 3.617(2)
		Ni(1)–Ni(3) 3.127(2)	
		Ni(2)–Ni(3) 3.140(2)	
		Ni(1)–Cl(1) 2.4482(8)	
		Ni(1)–Cl(3) 2.4741(8)	
		Ni(2)–Cl(1) 2.4367(9)	
		Ni(2)–Cl(3) 2.4694(8)	
		Ni(3)–Cl(1) 2.5246(8)	
		Ni(3)–Cl(3) 2.4305(9)	
Ni(1)–Cl(1) 2.423(2)	Ni(3)–Cl(5) 2.449(2)	Ni(1)–Cl(2) 2.4248(8)	Ni(4)–Cl(6) 2.4156(9)
Ni(1)–Cl(2) 2.478(3)	Ni(3)–Cl(6) 2.502(2)	Ni(1)–Cl(5) 2.4055(8)	Ni(4)–Cl(6)' 2.4403(9)
Ni(1)–Cl(3) 2.469(2)	Ni(3)–Cl(7) 2.430(2)	Ni(2)–Cl(2) 2.4335(8)	Ni(4)–Cl(54) 2.5343(9)
Ni(2)–Cl(1) 2.408(2)	Ni(4)–Cl(5) 2.419(2)	Ni(2)–Cl(4) 2.4265(9)	Ni(5)–Cl(54) 2.3028(9)
Ni(2)–Cl(2) 2.393(2)	Ni(4)–Cl(6) 2.412(2)	Ni(3)–Cl(5) 2.4304(9)	
Ni(2)–Cl(3) 2.431(2)	Ni(4)–Cl(7) 2.408(2)	Ni(3)–Cl(4) 2.4461(9)	
Ni(1)–Cl(4) 2.378(2)	Ni(3)–Cl(8) 2.381(2)		Ni(5)–Cl(51) 2.2357(10)
			Ni(5)–Cl(52) 2.2576(9)
			Ni(5)–Cl(53) 2.2623(10)
Ni(1)–N(2*A*) 2.059(7)	Ni(3)–N(2*C*) 2.066(7)	Ni(1)–N(2*A*) 2.050(2)	Ni(4)–N(2*D*) 2.092(3)
Ni(1)–N(5*A*) 2.057(7)	Ni(3)–N(5*C*) 2.053(8)	Ni(1)–N(5*A*) 2.034(2)	Ni(4)–N(5*D*) 2.062(3)
Ni(2)–N(2*B*) 2.088(7)	Ni(4)–N(2*D*) 2.059(6)	Ni(2)–N(2*B*) 2.047(2)	Ni(4)–N(1*S*) 2.055(3)
Ni(2)–N(5*B*) 2.089(6)	Ni(4)–N(5*D*) 2.083(7)	Ni(2)–N(5*B*) 2.037(3)	
		Ni(3)–N(2*C*) 2.044(3)	
		Ni(3)–N(5*C*) 2.074(2)	
Ni(2)–O(1) 2.114(7)	Ni(4)–O(2) 2.105(6)		
Angle, deg			
		Ni(1)Ni(2)Ni(3) 59.91(1)	
		Ni(2)Ni(3)Ni(1) 59.78(1)	
		Ni(3)Ni(1)Ni(2) 60.31(1)	
Cl(1)Ni(1)Cl(2) 84.17(9)	Cl(5)Ni(3)Cl(6) 83.77(7)	Cl(5)Ni(1)Cl(2) 160.41(3)	Ni(4)Cl(6)Ni(4)' 96.28(3)
Cl(1)Ni(1)Cl(3) 83.57(7)	Cl(7)Ni(3)Cl(5) 84.69(8)	Cl(2)Ni(2)Cl(4) 159.84(3)	Ni(4)Cl(54)Ni(5) 122.11(4)
Cl(3)Ni(1)Cl(2) 83.09(7)	Cl(7)Ni(3)Cl(6) 83.23(7)	Cl(4)Ni(3)Cl(5) 158.50(3)	
Cl(4)Ni(1)Cl(1) 92.95(8)	Cl(8)Ni(3)Cl(5) 94.84(8)		
Cl(4)Ni(1)Cl(2) 176.94(10)	Cl(8)Ni(3)Cl(6) 177.66(8)		
Cl(4)Ni(1)Cl(3) 97.64(7)	Cl(8)Ni(3)Cl(7) 94.79(8)		
Cl(1)Ni(2)Cl(3) 84.71(7)	Cl(6)Ni(4)Cl(5) 86.33(7)		
Cl(2)Ni(2)Cl(1) 86.36(8)	Cl(7)Ni(4)Cl(5) 85.83(8)		
Cl(2)Ni(2)Cl(3) 85.70(9)	Cl(7)Ni(4)Cl(6) 85.63(7)		
N(5*A*)Ni(1)N(2*A*) 79.1(3)	N(5*C*)Ni(3)N(2*C*) 77.8(3)	N(2*A*)Ni(1)N(5*A*) 80.55(10)	N(2*D*)Ni(4)N(5*D*) 79.74(10)
N(2*B*)Ni(2)N(5*B*) 78.8(3)	N(2*D*)Ni(4)N(5*D*) 79.3(2)	N(2*B*)Ni(2)N(5*B*) 80.51(10)	
		N(2*C*)Ni(3)N(5*C*) 80.45(10)	
Ni(2)Cl(1)Ni(1) 78.70(6)	Ni(4)Cl(5)Ni(3) 77.68(7)	Ni(1)Cl(2)Ni(2) 80.01(3)	Cl(6)Ni(4)Cl(6)' 83.72(3)
Ni(2)Cl(2)Ni(1) 77.90(6)	Ni(4)Cl(6)Ni(3) 76.79(6)	Ni(2)Cl(4)Ni(3) 80.23(3)	
Ni(2)Cl(3)Ni(1) 77.37(6)	Ni(4)Cl(7)Ni(3) 78.25(7)	Ni(3)Cl(5)Ni(1) 80.57(3)	

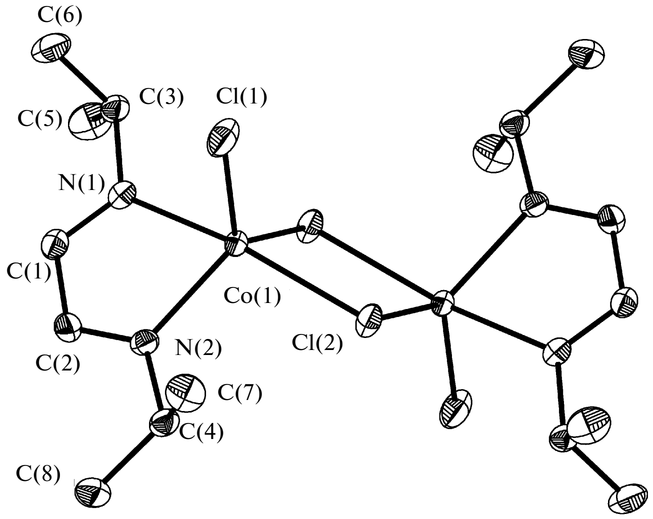

Fig. 2. Structure of complex **VIII** with the enumeration of atoms (independent part); hydrogen atoms are omitted.

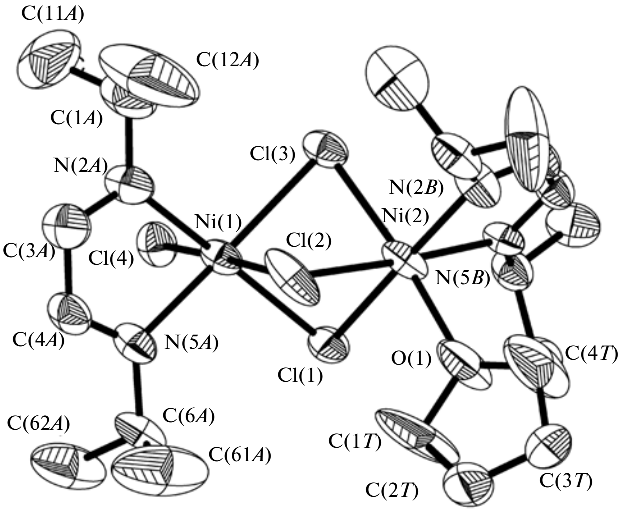

Fig. 3. Structure of complex **XII** with the enumeration of atoms. One of the crystallographically independent molecules is shown; hydrogen atoms are omitted.

were assigned on the basis of the spectrum of free $^{\mathrm{Me}}\mathrm{DAB}^{\mathrm{Mes}}$ described in the literature [18].

The Zn complexes with all ligands studied ($^{\mathrm{Me}}\mathrm{DAB}^{\mathrm{Mes}}$, $^{\mathrm{Me}}\mathrm{DAB}^{\mathrm{Dipp}}$, $^{\mathrm{H}}\mathrm{DAB}^{t\mathrm{Bu}}$, and $^{\mathrm{H}}\mathrm{DAB}^{i\mathrm{Pr}}$) are mononuclear. The coordination node ZnN_2Cl_2 in complexes **I–IV** has the structure of a distorted tetrahedron, and the dihedral angle between the ZnN_2 and $ZnCl_2$ planes varies from 85° to 90°. The molecular structure of complex **I** is shown in Fig. 1.

The Co complexes, except for complex **VIII** with $^{\mathrm{H}}\mathrm{DAB}^{i\mathrm{Pr}}$, are mononuclear. The structure of complex **V** turned out to be identical to the structure described earlier [19], and the unit cell parameters coincide with allowance for the temperature factor. Complex **VI** has earlier been characterized structurally as a solvate with methylene chloride **VI** · CH_2Cl_2 [19]. The average bond lengths Co–N (2.045 and 2.050 Å) and Co–Cl (2.22 and 2.20 Å) in **VI** and **VI** · CH_2Cl_2 are consistent with each other.

Another polymorphous modification (**VII'**) has earlier been described for compound **VII** [20]. The volume of the monoclinic unit cell in **VII'** is twofold lower than that observed for **VII**, and this unit cell is transformed into that similar to **VII** by the axis transformation matrix (–1 0 0/0 –1 0/0 0 2). The space group of **VII'** ($P2_1$) is the subgroup $P2_1/n$ in which structure **VII** is solved. An attempt to solve structure **VII** in the unit cell of **VII'** and space group $P2_1$ results in the high value of *R* factor (~11%). Thus, there is a topotaxial correspondence between these modifications. The IR spectra of complexes **V–VII** coincide with the published data.

The cobalt complex $[Co(^{\mathrm{H}}\mathrm{DAB}^{i\mathrm{Pr}})Cl_2]_2$ (**VIII**) has a centrosymmetric binuclear structure, and the Cl(1) atom performs the bridging function (Fig. 2). The coordination polyhedron of the Co atom is a slightly distorted trigonal bipyramid, whose equatorial positions are occupied by the N(2), Cl(1), and Cl(2) atoms. The deviation of the terminal chloride ion Cl(2) from the Co(1)Cl(2)Co(1)'Cl(2)' plane is 1.81 Å, and the dihedral angle between the Co(1)Cl(2)Co(1)'Cl(2)' and Co(1)N(1)C(1)C(2)N(2) planes is 55°. It should be mentioned that the monomeric structure with the tetrahedral coordination node has earlier been postulated for the complexes of stoichiometry $[Co(^{\mathrm{H}}\mathrm{DAB}^{i\mathrm{Pr}})Hal_2]$ (Hal = Cl, Br) on the basis of the UV spectra and magnetic susceptibility data, although the complexes were not characterized by X-ray structure analysis [20].

The crystals of the nickel complexes $[Ni(^{\mathrm{Me}}\mathrm{DAB}^{\mathrm{Dipp}})Cl_2]$ (**IX**) and $[Ni(^{\mathrm{Me}}\mathrm{DAB}^{\mathrm{Mes}})Cl_2]$ (**X**) are isostructural to the crystals of the corresponding cobalt complexes **V** and **VI**. Interestingly, the crystals of **IX** are also isostructural to the crystals of $[Co(^{\mathrm{H}}\mathrm{DAB}^{\mathrm{Dipp}})(CO)(NO)]$ [21] and $[Ni(^{\mathrm{H}}\mathrm{DAB}^{\mathrm{Dipp}})(CO)_2]$ [22] containing more bulky ligands CO or NO instead of halides and containing no methyl substituents in the side chain of DAB. Unlike mononuclear cobalt complex **VII**, the nickel complex with $^{\mathrm{H}}\mathrm{DAB}^{t\mathrm{Bu}}$ (**XI**) has the pseudosymmetric binuclear structure with two bridging Cl atoms. The central fragment Ni(1)Cl(1)Ni(2)Cl(3) is almost planar (the deviation of the atoms from the plane does not exceed 0.03 Å), and the dihedral angles between this fragment and the Ni(1)N(1*B*)C(2*B*)C(2*B*)N(2*B*) and Ni(2)N(1*A*)C(2*A*)C(2*A*)N(2*A*) planes are 78.0° and 77.9°, respectively. Unlike complex **VIII**, the coordination polyhedra in complex **XI** are similar to a square pyramid with a distorted base formed by three Cl atoms and one N atom. The deviation of the terminal chloride ions Cl(2) and Cl(4) from the

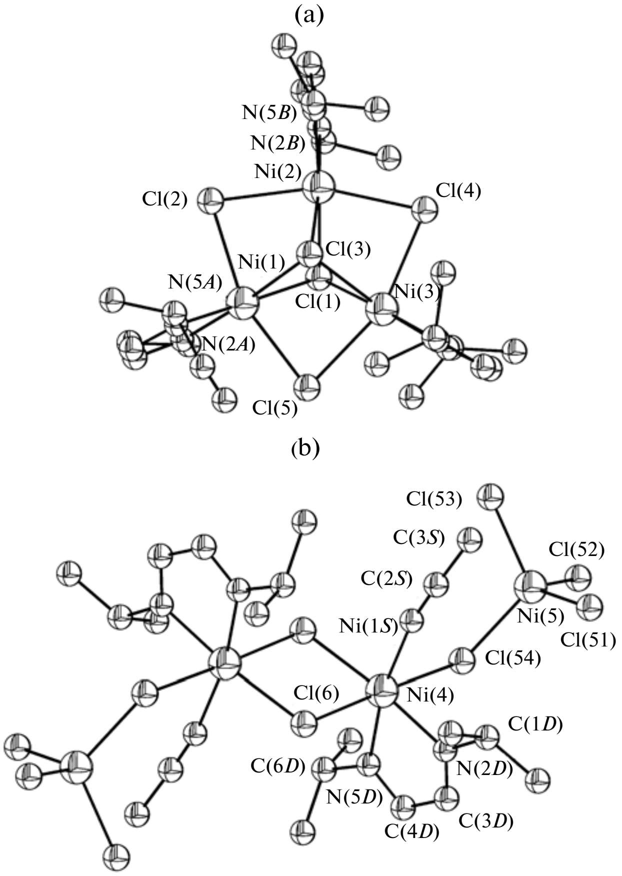

Fig. 4. Structures of the (a) anionic and (b) cationic parts of complex **XIII** with the enumeration of atoms of the independent part; hydrogen atoms are omitted.

Ni(1)Cl(1)Ni(2)Cl(3) plane is 0.88 and 0.93 Å, respectively.

Unlike binuclear complexes **VIII** and **XI**, complex **XII** ($Ni_2(\mu\text{-}Cl)_3({}^{H}DAB^{iPr})_2(THF)Cl]$) contains three bridging chloride ligands. The crystalline phase of the complex includes two crystallographically independent molecules. The coordination of the Ni atoms is supplemented to the octahedral one by diimine and one more terminal ligand (Cl for Ni(1) and Ni(3), THF for Ni(2) and Ni(4)). The molecular structure of complex **VIII** is shown in Fig. 3.

The crystalline phase of complex **XIII** consists of the complex cations $[Ni_3(\mu_3\text{-}Cl)_2(\mu\text{-}Cl)_3({}^{H}DAB^{iPr})_3]^+$ (**XIIIa**) (Fig. 4a), complex anions $[Ni_4Cl_{10}({}^{H}DAB^{iPr})_2(MeCN)_2]^{2-}$ (**XIIIb**) (Fig. 4b), and solvate acetonitrile molecules. The average Ni–Ni distance in **XIIIa** (3.13 Å) indicates the absence of binding between the metal ions. The Ni–(μ_3-Cl) and Ni–(μ-Cl) distances are 2.47(3) and 2.428(13) Å, respectively. Only two examples of complexes containing the $[Ni_3(\mu_3\text{-}Hal)_2(\mu\text{-}Hal)_3]$ fragment are described in the Cambridge Structural Database (CSD, version 5.32, November 2010): $[Ni_3(\mu_3\text{-}Cl)_2(\mu\text{-}Cl)_3(Tmeda)_3]^+$ (Tmeda is N,N,N',N'-tetramethylethylenediamine) [23] and the complex with the dimine ligand $[Ni_3(\mu_3\text{-}Br)_2(\mu\text{-}Br)_3({}^{Me}DAB^{Ar})_3]^+$ (Ar is 2-methyl-4-chlorophenyl) [24]. The geometric characteristics of cationic complex **XIIIa** are similar to those for $[Ni_3(\mu_3\text{-}Cl)_2(\mu\text{-}Cl)_3(Tmeda)_3]^+$: Ni–Ni 3.165, Ni–($\mu_3$-Cl) 2.427(2), Ni–($\mu$-Cl) 2.471(2) Å. The Ni–Br distances in the complex $[Ni_3(\mu_3\text{-}Br)_2(\mu\text{-}Br)_3({}^{Me}DAB^{Ar})_3]^+$ [24] are somewhat longer (Ni–(μ_3-Br) 2.549(3), Ni–(μ-Br) 2.595(3) Å), which can be explained by the longer ion radius of Br^-.

Complex anion **XIIIb** is a centrosymmetric dimer. Two μ-chloride ligands bind two Ni atoms. One ${}^{H}DAB^{iPr}$ molecule and one MeCN molecule are additionally coordinated to each Ni atom. In addition, the Ni(4) atom is bound through the bridging Cl(54) atom to the Ni(5) atom, which is in the tetrahedral coordination of four Cl atoms. Thus, it can be imagined that the complex fragment $NiCl_4^{2-}$ acts, in this case, as a ligand with respect to the Ni(4) atom. The search in the CSD [25] showed that this coordination mode of $NiHal_4^{2-}$ has not previously been known. On the one hand, the closest analogs of this structure are two complexes of the $[L_2Ni(\mu\text{-}Br)_2NiBr_2]$ type, where L is the bidentate-coordinated ligand [25, 26]. On the other hand, the examples for the $\{M^1\text{–}(\mu\text{-}Hal)\text{–}M^2Hal_3\}$ fragment (M^1 and M^2 are metals of the first transition row) are rather numerous (43 notations in the CSD). The Ni(4)–Ni(4)' distance in **XIIIb** is ~3.62 Å, and the Ni(4)–Ni(5) distance is ~4.23 Å.

The C–C and C–N bond lengths of the diimine fragment in all studied complexes range within 1.44–1.52 and 1.23–1.30 Å, respectively, which unambiguously indicates the zero oxidation state of the ligand.

ACKNOWLEDGMENTS

This work was supported by the Russian Foundation for Basic Research (project nos. 10-03-00385, 12-03-31530, and 12-03-90820), the Siberian Branch of the Russian Academy of Sciences (integration project nos. 17 and 105), and the state contract no. 02.740.11.0628.

REFERENCES

1. Johnson, L.K., Killian, C.M., and Brookhart, M., *J. Am. Chem. Soc.*, 1995, vol. 117, p. 6414.
2. Shaver, M.P., Allan, L.E.N., Rzepa, H.S., and Gibson, V.C., *Angew. Chem., Int. Ed.*, 2006, vol. 45, p. 1241.
3. Allan, L.E.N., Shaver, M.P., White, A.J.P., and Gibson, V.C., *Inorg. Chem.*, 2007, vol. 46, p. 8963.
4. Binotti, B., Carfagna, C., Zuccaccia, C., and Macchioni, A., *Chem. Commun.*, 2005, p. 92.
5. Sprengers, J.W., Greef, M., Duin, M.A., and Elsevier, C.J., *Eur. J. Inorg. Chem.*, 2003, p. 3811.

6. Heumann, A., Giordano, L., and Tenaglia, A., *Tetrahedron Lett.*, 2003, vol. 44, p. 1515.
7. Liu, Y., Li, S., Yang, X.-J., et al., *Organometallics*, 2009, vol. 28, p. 5270.
8. Kreisel, K.A., Yap, G.P.A., Dmitrenko, O., et al., *J. Am. Chem. Soc.*, 2007, vol. 129, p. 14162.
9. Hsieh, A.T.T. and West, B.O., *J. Organomet. Chem.*, 1976, vol. 112, p. 285.
10. Ward, L.G.L., *Inorg. Synt.*, 1972, vol. 13, p. 154.
11. Gordon, A. and Ford, R., *The Chemist's Companion: A Handbook of Practical Data, Techniques, and References*, New York: Wiley, 1972.
12. Sheldrik G.M., *SADABS. Program for Empirical X-ray Absorption Correction Bruker*, 1990–2010.
13. *SHELXTL. Version 6.22*, Madison (WI, USA): Bruker AXS Inc., 2005.
14. Turki, T., Guerfel, T., and Bouachir, F., *Inorg. Chem. Commun.*, 2006, vol. 9, p. 1023.
15. Kreisel, K.A., Yap, G.P.A., and Theopold, K.H., *Inorg. Chem.*, 2008, vol. 47, p. 5293.
16. Malkov, A.E., Fomina, I.G., Sidorov, A.A., et al., *J. Mol. Struct.*, 2003, vol. 656, p. 207.
17. Hierso, J.-C., Ellis, D.D., Spek, A.L., et al., *Chem. Commun.*, 2000, p. 1359.
18. Schaub, T. and Radius, U., *Z. Anorg. Allg. Chem.*, 2006, vol. 632, p. 807.
19. Rosa, V., Gonzalez, P.J., Avilés, T., et al., *Eur. J. Inorg. Chem.*, 2006, p. 4761.
20. Barral, M.C., Delgado, E., and Gutiérrez-Puebla, E., *Inorg. Chim. Acta*, 1983, vol. 74, p. 101.
21. Sieger, M., Hübler, K., Scheiring, T., et al., *Z. Anorg. Allg. Chem.*, 2002, vol. 628, p. 2360.
22. Schleis, T., Spaniol, T.P., Okuda, J., et al., *J. Organomet. Chem.*, 1998, vol. 569, p. 159.
23. Handley, D.A., Hitchcock, P.B., and Leigh, G.J., *Inorg. Chim. Acta*, 2001, vol. 314, p. 1.
24. Helldörfer, M., Backhaus, J., Milius, W., and Alt, H.G., *J. Mol. Catal.*, 2003, vol. 193, p. 59.
25. Winston, S., Stylianides, N., Tulloch, A.A.D., et al., *Polyhedron*, 2004, vol. 23, p. 2813.
26. Wang, Y., Lin, S., Zhu, F., et al., *Inorg. Chim. Acta*, 2009, vol. 362, p. 166.